NASA Technical Memorandum 103781
ICOMP-91-04

A 2-D Oscillating Flow Analysis in Stirling Engine Heat Exchangers

Kyung H. Ahn
Institute for Computational Mechanics in Propulsion
Lewis Research Center
Cleveland, Ohio

and

Mounir B. Ibrahim
Cleveland State University
Cleveland, Ohio

Prepared for the
1991 Joint ASME-JSME Fluids Engineering Conference
Portland, Oregon, June 24-26, 1991

NASA

INSTITUTE FOR COMPUTATIONAL MECHANICS IN PROPULSION
NASA LEWIS RESEARCH CENTER
ICOMP
CASE WESTERN RESERVE UNIVERSITY

A 2-D OSCILLATING FLOW ANALYSIS IN STIRLING ENGINE HEAT EXCHANGERS

Kyung H. Ahn
Institute for Computational Mechanics in Propulsion
NASA Lewis Research Center, MS 5-3
21000 Brookpark Road
Cleveland, Ohio 44135

and

Mounir B. Ibrahim
Department of Mechanical Engineering
Cleveland State University
Cleveland, Ohio 44115

ABSTRACT

A two dimensional oscillating flow analysis has been conducted simulating the gas flow inside Stirling engine heat exchangers. Both laminar and turbulent oscillating pipe flow has been investigated numerically for Re_{max}=1920 (Va = 80), 10800 (Va = 272), 19300 (Va = 272), 60800 (Va = 126). The results are compared with experimental results of previous investigators. Also predictions of the flow regime on present oscillating flow conditions have been checked by comparing velocity amplitudes and phase difference with those from laminar theory and quasi-steady profile. A high Reynolds number $k-\epsilon$ turbulence model was used for turbulent oscillating pipe flow. Finally, performance evaluation of the $k-\epsilon$ model was made to explore the applicability of quasi-steady turbulent models to unsteady oscillating flow analysis.

NOMENCLATURE

c_μ = coefficient used in eddy viscosity equation
c_{ϵ_i} = turbulence model constants for ϵ equation (i=1,2)
D = diameter of the pipe, m
k = turbulent kinetic energy, m^2/s^2, $[= 1/2\,(\overline{u'^2}+\overline{v'^2}+\overline{w'^2})]$
l = turbulence length scale, m
l_m = mixing length, m, $(=\kappa y)$
L = length of the pipe, m
P = pressure, N/m^2
r = radial coordinate, m
R = radius of the pipe, m
Re_{max} = Reynolds number, $(= |u_m| \cdot D/\nu)$
t = time, s
u = axial velocity, m/s
$|u|$ = amplitude of axial velocity, m/s
$\mathbf{v}$ = velocity vector, m/s
Va = Valensi number (dimensionless frequency), $(= \omega \cdot R^2/\nu)$
x = axial coordinate, m
δ = Stokes-layer thickness, $m/rad^{1/2}$, $[= (2\nu/\omega)^{\frac{1}{2}}]$
ϵ = dissipation rate of turbulent kinetic energy, m^2/s^3
λ = friction factor
η = dimensionless radial coordinate, (r/R)
μ = viscosity, Ns/m^2
ν_f = kinematic viscosity, m^2/s
ρ = density, kg/m^3
σ_k = turbulent Prandtl number for k equation
σ_ϵ = turbulent Prandtl number for ϵ equation
τ = shear stress, N/m^2
ω = angular frequency, rad/s

Superscripts
$\bar{}$ = time averaged value
$'$ = fluctuating velocity component

Subscripts
c = critical value
cl = values at a pipe centerline
i,j = denotes spatial coordinates [$=(r,\theta,x)$]
m = cross-sectional mean value
w = value at pipe wall

INTRODUCTION

The problems of periodic turbulent internal flow has been studied by many research workers experimentally as well as computationally (1-8). The periodic flow can be divided into two classes:1) unsteady flow with non-zero mean velocity and 2) unsteady flow with zero mean velocity. Previous researchers have called the first class of periodic flow, pulsating flow, and the second class, oscillating flow.

The effect of imposed periodic pulsations on the time-averaged properties has been previously investigated. Ramaprian and Tu (1) found that for sufficiently high frequencies, the time-averaged flow variables, e.g., velocity, wall shear stresses and power loss due to friction, were affected by the imposed unsteadiness. They also concluded that, from their computations, a quasi-steady turbulence model cannot adequately describe unsteady flow conditions, at least for high frequencies. Ohmi et al. (3) performed extensive pulsating flow experiments to determine transition criteria via non-dimensional parameters on the basis of velocity measurements. The early investigation of Sarpkaya (5), by detecting the growth rate of artificial disturbances, and Hershey and Im (6), by friction factor measurements, show that critical

Reynolds number $Re_{max,c}$ is much different from the steady-flow value of about 2300.

Hino et al. (7, 8) investigated oscillating turbulent flow in pipes and rectangular ducts experimentally for various Reynolds numbers and frequencies. Many useful turbulent flow data have been generated through their work. They found that the turbulent energy production becomes exceedingly high in the decelerating phase, but the turbulence is reduced to a very low level at the end of the decelerating phase and in the accelerating stage of reversal flow.

So far, no extensive numerical calculations have been given for oscillating flows covering wide ranges of Reynolds number and frequencies. Köhler (9) has performed numerical simulations of turbulent oscillating flows and compared mean velocity profiles and fluctuations with experimental results which were obtained from the oscillating flow test facility at the University of Minnesota [see Seume and Simon (10)].

In the present paper, turbulent oscillating pipe flow has been analyzed by solving time-averaged continuity and momentum equations using the standard $k-\epsilon$ turbulence model of Launder and Sparding (11). A computer code, CAST, developed by Perić and Scheuerer (12), has been modified to handle unsteady inlet conditions. Since most constants for this $k-\epsilon$ model originated from steady turbulent flow measurements together with simplified assumptions, the validity of this quasi-steady turbulence model for unsteady flow conditions has been questioned. Performance evaluation of this $k-\epsilon$ model for the present oscillating flow conditions will be discussed; One objective is to check the applicability of this quasi-steady turbulent model to oscillating flow analysis.

ANALYSIS

Governing Equations and Numerical Scheme

The time-averaged equations of continuity and motion for an unsteady Newtonian fluid with constant fluid properties can be written as follows in vector form.

Equation of continuity:

$$(\nabla \cdot \mathbf{v}) = 0 \tag{1}$$

Equation of motion:

$$\rho \frac{D\mathbf{v}}{Dt} = -\nabla \mathbf{P} - [\nabla \cdot \vec{\tau}] \tag{2}$$

In handling turbulent flow conditions, the above dependent variables represent time-averaged values and turbulent shear stress term in Equation (2) is closed by the "high Reynolds number version" of k-ϵ turbulence model which requires solutions of the following transport equations:

$$\rho \frac{Dk}{Dt} = (\mu_t/\sigma_k)\left[\nabla^2 k\right] + P - \rho\epsilon \tag{3}$$

$$\rho \frac{D\epsilon}{Dt} = (\mu_t/\sigma_\epsilon)\left[\nabla^2 \epsilon\right] + \frac{\epsilon}{k}(c_{\epsilon_1} P - c_{\epsilon_2}\rho\epsilon) \tag{4}$$

The present $k-\epsilon$ model has the eddy viscosity given by

$$\mu_t = c_\mu \rho \frac{k^2}{\epsilon} \tag{5}$$

and the production rate of turbulent kinetic energy is given by

$$P = -\rho\overline{(u_i' u_j')} \frac{\partial u_i}{\partial x_j} \tag{6}$$

The empirical constants are the standard values, $c_\mu = 0.09$, $c_{\epsilon_1} = 1.44$, $c_{\epsilon_2} = 1.92$, $\sigma_k = 1.0$, $\sigma_\epsilon = 1.3$. The wall function method is used to specify wall boundary conditions.

A conservative finite volume method with collocated variable arrangement by Perić et al. (13) is used for discretization. The convection fluxes in the model transport equations are discretized with the first-order upwind differencing scheme. Central differences are used to approximate the diffusion fluxes.

Boundary and Initial Conditions

Particular attention was paid to a flow geometry used by previous workers to perform the experimental oscillating flows; see Ohmi et al. (3). The flow geometry is a circular pipe, as shown in Figure (1), with diameter of 50.4 mm and length of 6000 mm; This gives $L/D \simeq 60$ at the middle section of the pipe. At this middle section the flow can be considered fully developed. The inflow is taken to be uniform over the cross section and time dependent according to the relation:

$$u_{m,in} = |u_m| \sin\omega t \tag{7}$$

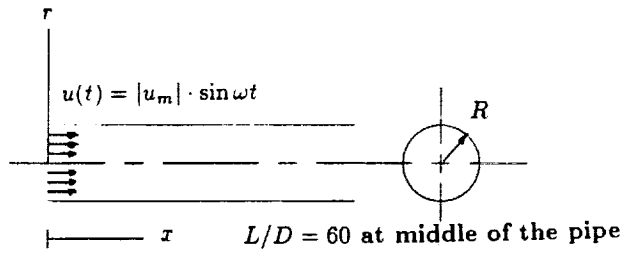

Fig. 1 Geometry of the pipe and inlet condition for oscillating flow

FLOW COMPUTATIONS AND RESULTS

Four cases have been studied for $2000 \leq Re_{max} \leq 60000$ with different oscillating frequencies [see Table (1)]. 62 × 22 grid nodes were used in the axial and radial directions respectively. A grid independence test has been carried out by doubling the grid nodes. For each case, 180 time steps were used in one cycle and the results were collected after 4 consecutive cycles. Convergence criteria has been set to 0.1% of the residual norms for every dependent variable and about 2000 seconds of CPU time (Cray XMP) per cycle has been obtained.

Ohmi et al. (14) derived the following critical Reynolds number, for fully developed flow, up to which the theoretical correlation for laminar oscillating flow is valid.

$$\frac{Re_{max,c}}{\sqrt{Va}} = 882 \tag{8}$$

According to equation (8), Cases 1 and 2 are in laminar regime and Cases 3 and 4 fall into the turbulent regime [see Table (I)]. In the following sections, computational results for fully developed oscillating flow are analyzed for each test case by comparing with both experimental data (3, 14) and steady state analyses.

Table I An outline of test cases

Testcase	Re_{max}	Va	$Re_{max}/(Va)^{1/2}$	$Re_{max}/(Va)^{1/2}$ Eqn. (8)	Eqn. (17)	Hino et al.(8)
Case 1	1920	80	215	882	620	770
Case 2	10800	272	655		676	
Case 3	19300	272	1171		676	
Case 4	60800	126	5409		640	

Calculation of Oscillating Flow in Laminar Regime

Figures (2a) and (2b) show the instantaneous velocity versus ωt at different radial locations for Cases 1 and 2 respectively. The plots in those figures are made for the axial location at the middle of the pipe. The plots show the increase in the velocity amplitude as the distance from the wall increases; also shown on the plot are differences in phase angle between the fluid motion near the wall and that near the pipe center line. Profiles of the velocity amplitude normalized by the center line value versus normalized radial distance for Case 1 and 2 are shown in Figures (3a) and (3b). Also shown on the plots are the phase differences between the velocity at any radial position and that of the center line. In those Figures, Ohmi's experimental data (3) for both amplitude ratio and phase differences are shown and an excellent agreement was obtained except, near the pipe wall large discrepancies in phase differences are noticed. It was found that, from laminar theory, phase difference increases rapidly as approaching the pipe wall and present numerical results follows the trend of laminar theory [see Figures (3a) and (3b)] and the same deviation was found in earlier work between experimental and laminar theory [see (3)]. Consequently, the above discrepancies near the wall for phase differences can be attributed to difficulties in near-wall measurement. In Figure (3b), the dashed line represents steady turbulent velocity profile (1/7 power law). This shows that Case 2, although on the borderline between laminar/turbulent regime, is very close to laminar flow condition and still away from turbulent motion [see Figure (6)].

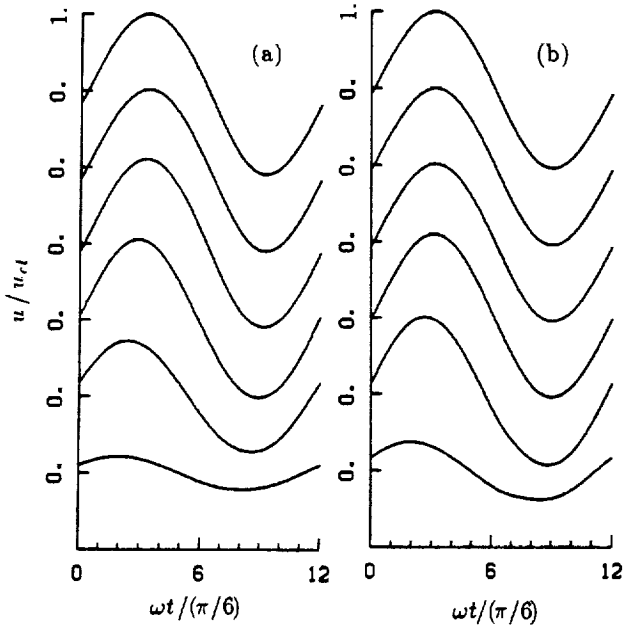

Fig. 2 Laminar axial velocity distribution versus crank angle during a cycle
(a) Case 1
(b) Case 2

(Data were obtained at r/R = 0, 0.25,0.55, 0.75, 0.88, 0.97 from top to bottom respectively.)

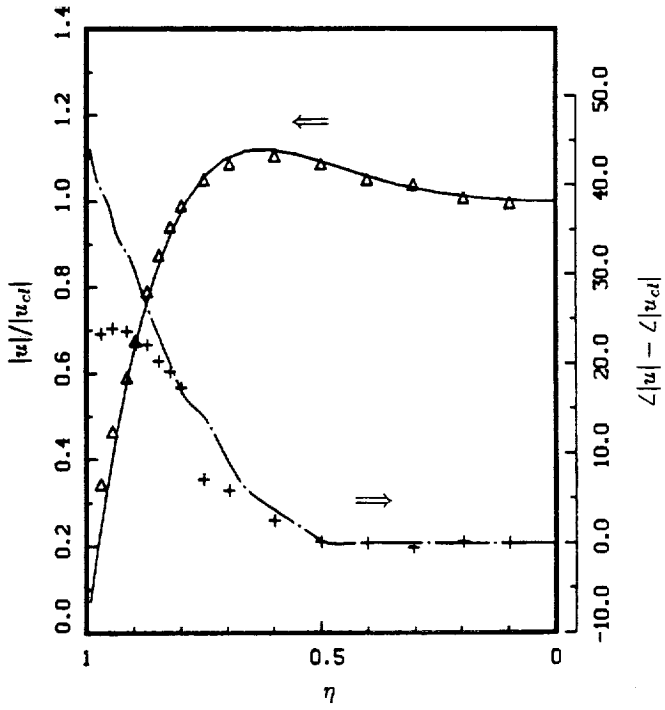

Fig. 3a Profile of the velocity amplitude and phase difference for Case 1

(Velocity amplitude:
solid line; present numerical data,
△ △ △; experimental data,
Phase difference:
chain dot line; present numerical data,
+ + +; experimental data.)

Calculation of Oscillating Flow in Turbulent Regime

Calculation were also made for oscillating flow in the turbulent regime. Inlet turbulent kinetic energy k_{in} was obtained assuming isotropic turbulence:

$$k_{in} = \frac{3}{2}(TI \times u_{m,in})^2 \tag{9}$$

where TI is turbulent intensity at the inlet which is assumed to be 1% for Cases 3 and 4. Also the turbulence length scale at the inlet l_{in} was approximated by the following equation [see Perić and Scheuerer (12)]:

$$l_{in} = \frac{k_{in}^{3/2}}{\epsilon_{in}} \tag{10}$$

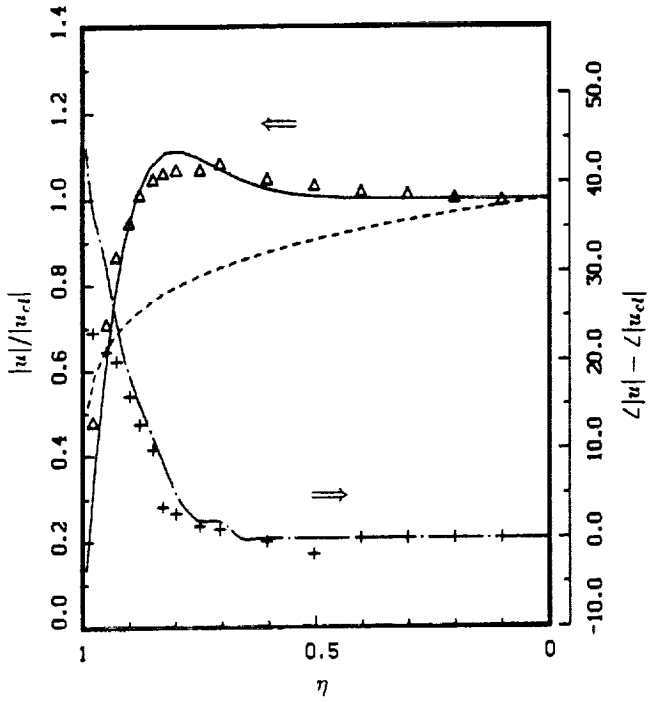

Fig. 3b Profile of the velocity amplitude and phase difference for Case 2

(Velocity amplitude:
solid line; present numerical data.
dashed line; 1/7 power law profile,
△ △ △; experimental data,
Phase difference:
chain dot line; present numerical data.
+ + +; experimental data.)

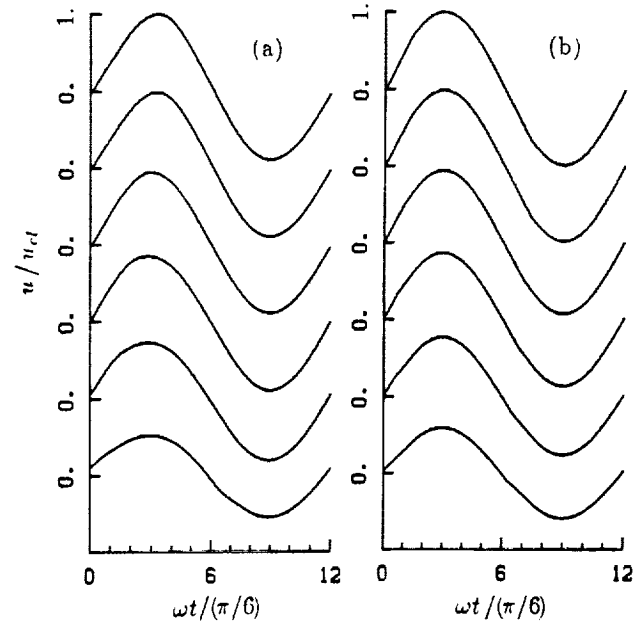

Fig. 4 Turbulent axial velocity distribution versus crank angle during a cycle
(a) Case 3
(b) Case 4

(Data were obtained at r/R = 0, 0.25,0.55, 0.75, 0.88, 0.97 from top to bottom respectively.)

Equation (10) holds under local equilibrium conditions and for a logarithmic velocity law [see Rodi (15)] and in the equation, the turbulent dissipation rate ϵ_{in} was estimated from Equation (5):

$$\epsilon_{in} = c_\mu \rho \frac{k_{in}^2}{\mu_{t,in}} \tag{11}$$

The following assumption for turbulent viscosity [Köhler (9)] was used:

$$\mu_{t,in} = \sqrt{Re_{max}}\, c_\mu \mu \tag{12}$$

Then Equation (11), after substituting Equation (12), becomes

$$\epsilon_{in} = \frac{1}{\sqrt{Re_{max}}} \frac{k_{in}^2}{\nu} \tag{13}$$

With the above relationships, turbulence length scale was estimated about 20% of the pipe diameter.

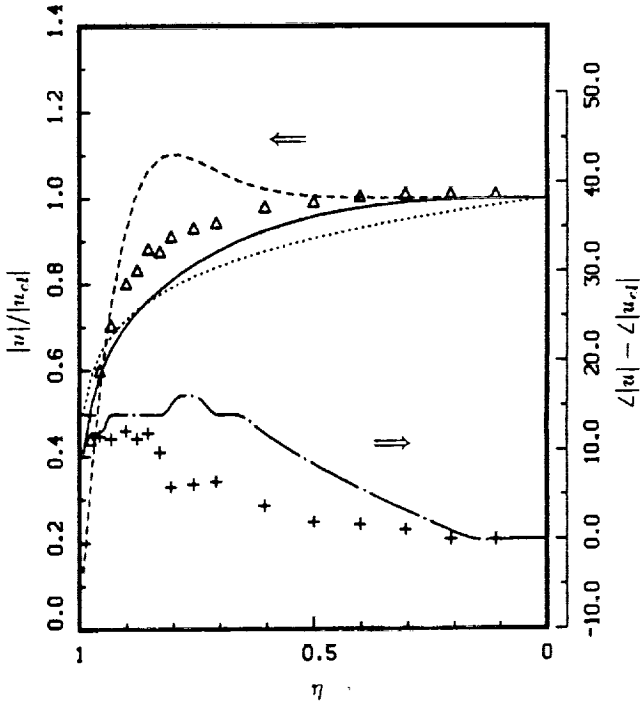

Fig. 5a Profile of the velocity amplitude and phase difference for Case 3

(Velocity amplitude:
solid line; present numerical data,
dashed line; laminar profile,
dotted line; 1/7 power law profile,
△ △ △; experimental data,
Phase difference:
chain dot line; present numerical data,
+ + +; experimental data.)

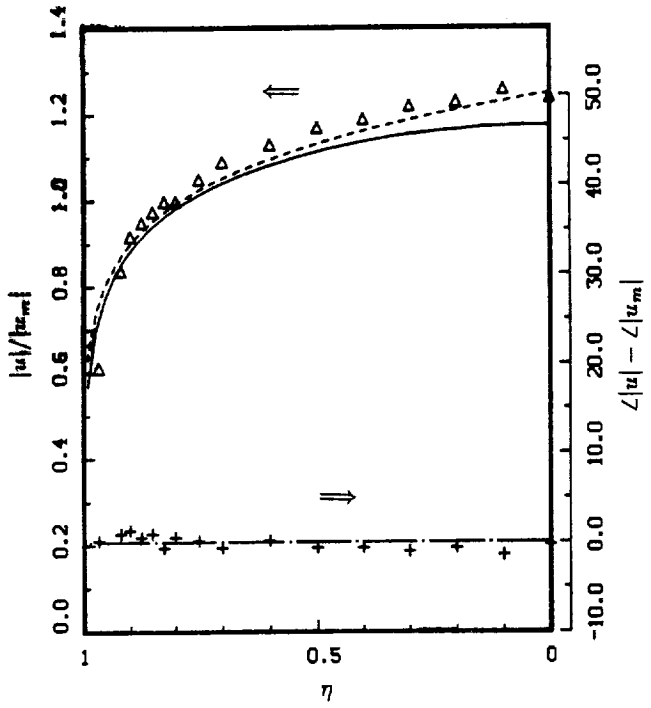

Fig. 5b Profile of the velocity amplitude and phase difference for Case 4

(Velocity amplitude:
solid line; present numerical data,
dashed line; 1/7 power law profile,
△ △ △; experimental data,
Phase difference:
chain dot line; present numerical data,
+ + +; experimental data.)

Computational results are shown in Figures (4) and (5) in the same order as in the laminar cases. Figures (4a) and (4b) show the time averaged velocity versus ωt at different radial location for Cases 3 and 4 respectively. The plots show, in contrast with the laminar cases, much less variation in velocity phase with radial position. Specially, in Figure 4b, it is noticed that no phase differences are shown across the pipe cross section. Also profiles of the normalized velocity amplitude versus normalized radial distance for Cases 3 and 4 are shown in Figures (5a) and (5b). Also shown on the plots are the phase difference between the velocity amplitudes. It should be noted that in Case 4 the normalized velocity was obtained using the amplitude of the "cross-sectional mean" velocity (rather than the center line one - used in Cases 1, 2, and 3). Also, the phase differences in Case 4 was obtained from the difference between the velocity at any radial position and the "cross-sectional mean" velocity (rather than the center line one - used in Case 1, 2, and 3).

Experimental results for Case 3 indicate that there are turbulent bursts in decelerating phase near the wall (3). As seen in Figure (5a), numerical results for both velocity amplitude ratio and velocity phase differences are different appreciably from the experimental data with maximum error of 14% and 40% respectively . Also, on Figure (5a), two reference plots are shown for the normalized velocity, one for laminar flow (dashed line) and the other for 1/7 power law profile (dotted line). It can be seen that the velocity amplitude ratio obtained numerically (solid line) nearly matches with 1/7 power law profile. Experimental data show intermediate value between the laminar and turbulent calculations in Figure (5a). Consequently, it indicates that the flow regime for Case 3 is in between laminar and turbulent (i.e., transient regime) and present high Reynolds number $k-\epsilon$ turbulence model does not adequately predict the oscillating fluid motion in this regime. In Case 4, experimental results show turbulent bursts on the velocity distributions during most of the cycle and agree well with steady turbulent correlation (14).

In Figure (5b), numerical results also shows good agreement with experimental data (< 7%). Specially, in Figures (4b) and (5b), both computation and data agree that the velocity phase remains nearly constant. Consequently, it is concluded that the flow regime for Case 4 reaches the fully turbulent regime or turbulent quasi-steady state as mentioned by earlier researchers.

CRITICAL REYNOLDS NUMBER

Hino et al. (8) summarized the critical Reynolds number from several experimental and theoretical results. From his work, two critical Reynolds numbers were found for the oscillating pipe flow. Experimental critical Reynolds numbers are found for Re_δ based on Stokes-layer thickness $\delta = (2\nu/\omega)^{\frac{1}{2}}$ and the cross-sectional mean velocity amplitude $|u_m|$ which can be expressed in terms of Re_{max} and Va as in Equation (8):

$$\frac{Re_{max,c}}{\sqrt{Va}} = \sqrt{2}\,\frac{|u_m|\delta}{\nu} = \sqrt{2}\,Re_{\delta,c} \tag{14}$$

Using visualization and power measurement technique, Sergeev (16) has determined critical Reynolds number to be $Re_{\delta,c} = 500$ and also using hot wire measurement, Hino et al. (8) obtained $Re_{\delta,c} = 550$; these result in values for $Re_{max,c}/\sqrt{Va}$ equal 710 and 770 respectively. As mentioned earlier, Ohmi et al. (14) predicted a value of 882 [Equation (8)]. They also derived another expression for critical Reynolds number using, instead of laminar oscillating flow theory, the following steady turbulent correlation together with the turbulence generation region assumption which was mentioned previously:

$$\left.\begin{aligned} \tau_w &= \lambda\,\rho\,|u_m|^2/8 \\ \lambda &= 0.3164/Re_{max}^{1/4} \end{aligned}\right\} \tag{15}$$

and obtained the following expression for critical Reynolds number:

$$Re_{max,c} = (211\sqrt{Va})^{8/7} \tag{16}$$

or

$$\frac{Re_{max,c}}{\sqrt{Va}} = (211)^{8/7}\,\sqrt{Va}^{1/7} \tag{17}$$

in terms of the expression of Equation (14). The above critical Reynolds numbers are tabulated for each case in Table I. Table I shows the flow conditions for each case examined in this paper as well as the estimated values of $Re_{max,c}/\sqrt{Va}$ by different investigators.

Also, plotted on Figure(6)are $\sqrt{Va}$ versus Re_{max} showing the four cases examined in this study, as well as Equations (8) and (17). From Figure (6), it is shown that Case 1

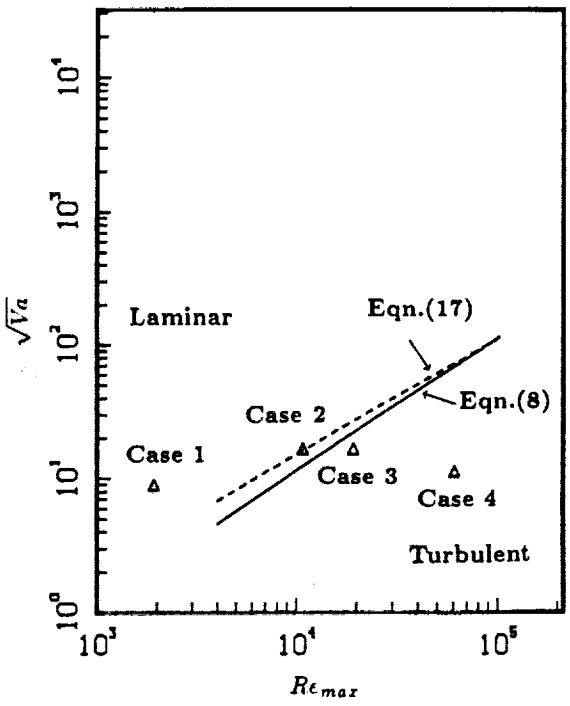

Fig. 6 Oscillating flow regime and critical Reynolds number.

is laminar and Case 4 is turbulent according to available correlations [Eqn. (8), (17)]. This finding is in agreement with the present numerical calculations. Case 2 is in the laminar flow regime according to Equation (8) and lies at the critical line [Eqn. (17)]: the present analysis shows that Case 2 is laminar. Case 3 is in the turbulent flow regime according to Equations (8) and (17), however the current analysis shows that it lies in between laminar and turbulent. More extensive computation will be conducted to complete the map shown in Figure (6) from computational point of view as well as experimental data available today.

SUMMARY AND CONCLUSIONS

Numerical calculations have been performed for oscillating flows in laminar, transition and turbulent regimes and comparisons have been made with experimental data. For turbulent computations, Launder-Spalding $k-\epsilon$ turbulence model has been employed with standard values of the model constants. The calculation method for the inlet values of turbulent kinetic energy k and turbulent length scale l has been discussed. Finally, several criteria for defining critical Reynolds number for oscillating pipe flow have been reviewed and compared according to the present numerical results. The conclusions for the results of the present investigation are given below:

[1] Oscillating flow in laminar flow regime can be simulated numerically with relatively high accuracy.

[2] Standard version of $k-\epsilon$ turbulence model cannot adequately model oscillating flow in transition flow regime.

[3] For fully turbulent regime or quasi-steady turbulent regime, the standard version of $k-\epsilon$ turbulence model can predict the oscillating flow within an allowable error.

[4] Critical Reynolds number defined by Ohmi et al. (14) from his experimental results seems to be reliable one from numerical calculations, however, since definition of transition region is not clear and also present numerical test data are scarce, extensive computations are needed to establish more reliable criteria for Stirling engine applications.

[5] For more rigorous numerical calculation for the oscillating flow in transition regime which is the case for most Stirling Cycles, further improvement in turbulence modeling is also necessary.

Acknowledgements – The authors would like to express their thanks to Mr. Roy Tew of NASA Lewis Research Center for valuable discussion on this paper.

REFERENCES

1. Ramaprian, B. R., and Tu, S. W., "Fully Developed Periodic Turbulent Pipe Flow. Part2, The Detailed Structure of the Flow," Journal of Fluid Mechanics, Vol. 137, 1983, pp. 59-81.

2. Mizushina, T., Maruyama, T., and Hirasawa, H., "Structure of Turbulence in Pulsating Pipe Flows," Journal of Chemical Engineering Japan, Vol. 8, 1975. pp. 210-216.

3. Ohmi, M., Iguchi, M., and Urahata I., "Transition to Turbulence in a Pulsatile Pipe Flow. Part 1. Wave Forms and Distribution of Pulsatile Velocities near Transition Region." Bulletin of JSME, Vol. 25, No. 200, February 1982, pp.182-189.

4. Ohmi, M., Iguchi, M., and Urahata I., "Flow Patterns and Frictional Losses in an Oscillating Pipe Flow," Bulletin of JSME, Vol. 25, No. 202, April 1982. pp. 536-543.

5. Sarpkaya. T., Transactions of ASME, Ser.D, Vol. 88, No. 3, 1966, pp. 589.

6. Hershey, D. and Im, C. S., AIChE Journal, Vol. 14, No. 5. 1968, pp. 807.

7. Hino, M., Kashiwayanagi, M., Nakayama A., and Hara, T., "Experiments on the Turbulence Statistics and the Structure of a Reciprocating Oscillatory Flow," Journal of Fluid Mechanics, Vol. 131, 1983, pp. 363-400.

8. Hino, M., Sawamoto, M., and Takasu, S.., "Experiments on the Transition to turbulence in an oscillatory pipe flow," Journal of Fluid Mechanics, Vol. 131, 1983, pp. 363-400.

9. Köhler, W. J., "Numerical Prediction of Turbulent Oscillating Flow and Associated Heat Transfer," Ph.D thesis. January 1990, University of Minnesota.

10. Seume, J. R., and Simon, T. W., "Oscillating Flow in Stirling Engine Heat Exchangers," Proc. of 21st Intersociety Energy Conversion Engineering Conf., IECEC Paper 869118, 1986, pp.533-538.

11. Launder, B. E., and Spalding, D. B.,"The Numerical Computation of Turbulent Flows", Computer Methods in Applied Mechanics and Engineering, Vol. 3, 1974, pp. 269-289.

12. Perić, M., and Scheuerer, G., "CAST - A Finite Volume Method for Predicting Two-Dimensional Flow and Heat Transfer Phenomena," GRS Technical Notes SRR-89-01, September 1989.

13. Perić, M., Rüger, M., and Scheuerer, G., "A Finite Volume Multigrid Method for Calculating Turbulent Flows," Proc. of Seventh Symp. on Turbulent Shear Flows, Paper 7-3, Stanford University, August 1989, pp.7.3.1-7.3.6.

14. Ohmi, M., and Iguchi, M., "Critical Reynolds Number in an Oscillating Pipe Flow," Bulletin of JSME, Vol. 25, No. 200, February 1982, pp. 165-172.

15. Rodi, W.,"Turbulence Models and Their Application in Hydraulics," Int. Association of Hydraulic Research Publ., Delft.

16. Sergeev, S. I., "Fluid Oscillations in Pipes at Moderate Reynolds Numbers," Fluid Dynamics, Vol. 1, 1966, pp. 21-22.

NASA
National Aeronautics and Space Administration

Report Documentation Page

1. Report No.	2. Government Accession No.	3. Recipient's Catalog No.
NASA TM - 103781 ICOMP - 91 - 04		

4. Title and Subtitle
A 2-D Oscillating Flow Analysis in Stirling Engine Heat Exchangers

5. Report Date

6. Performing Organization Code

7. Author(s)
Kyung H. Ahn and Mounir B. Ibrahim

8. Performing Organization Report No.
E - 6055

10. Work Unit No.
505 - 62 - 21

9. Performing Organization Name and Address
National Aeronautics and Space Administration
Lewis Research Center
Cleveland, Ohio 44135 - 3191

11. Contract or Grant No.

13. Type of Report and Period Covered
Technical Memorandum

12. Sponsoring Agency Name and Address
National Aeronautics and Space Administration
Washington, D.C. 20546 - 0001

14. Sponsoring Agency Code

15. Supplementary Notes
Prepared for the 1991 Joint ASME-JSME Fluids Engineering Conference, Portland, Oregon, June 24 - 26, 1991. Kyung H. Ahn, Institute for Computational Mechanics in Propulsion, Lewis Research Center (work funded by Space Act Agreement C - 99066 - G). Space Act Monitor: Louis A. Povinelli, (216) 433 - 5818. Mounir B. Ibrahim, Dept. of Mechanical Engineering, Cleveland State University, Cleveland, Ohio 44115.

16. Abstract
A two dimensional oscillating flow analysis has been conducted simulating the gas flow inside Stirling engine heat exchangers. Both laminar and turbulent oscillating pipe flow has been investigated numerically for Re_{max} = 1920 (Va = 80), 10800 (Va = 272), 19300 (Va = 272), 60800 (Va = 126). The results are compared with experimental results of previous investigators. Also predictions of the flow regime on present oscillating flow conditions have been checked by comparing velocity amplitudes and phase difference with those from laminar theory and quasi-steady profile. A high Reynolds number k - ε turbulence model was used for turbulent oscillating pipe flow. Finally, performance evaluation of the k - ε model was made to explore the applicability of quasi-steady turbulent models to unsteady oscillating flow analysis.

17. Key Words (Suggested by Author(s))	18. Distribution Statement
Oscillating flow; Stirling engine; Turbulent flow; k - ε turbulence model; Transition; Critical Reynolds number	Unclassified - Unlimited Subject Category 34

19. Security Classif. (of the report)	20. Security Classif. (of this page)	21. No. of pages	22. Price*
Unclassified	Unclassified		

*For sale by the National Technical Information Service, Springfield, Virginia 22161